Title

LONGITUDINAL STRUCTURAL CHANGES IN LATE-ONSET RETINAL DEGENERATION

Journal

Retina, 36(12)

ISSN

0275-004X

Authors

Cukras, Catherine
Flamendorf, Jason
Wong, Wai T
et al.

Publication Date

2016-12-01

DOI

10.1097/iae.0000000000001113

Peer reviewed

HHS Public Access

Author manuscript

Retina. Author manuscript; available in PMC 2017 December 01.

Published in final edited form as:

Retina. 2016 December ; 36(12): 2348–2356. doi:10.1097/IAE.0000000000001113.

Longitudinal Structural changes in Late-onset Retinal Degeneration

Catherine Cukras[1], **Jason Flamendorf**, **Wai T Wong**, **Radha Ayyagari**, **Denise Cunningham**, and **Paul A. Sieving**

[1]National Eye Institute, NIH Bethesda, Maryland 20892, USA

Abstract

Purpose—To characterize longitudinal structural changes in early stages of late-onset retinal degeneration (L-ORD) to investigate pathogenic mechanisms.

Methods—Two affected siblings, both with a S163R missense mutation in the causative gene C1QTNF5, were followed for 8+ years. Color fundus photos, fundus autofluorescence (FAF) images, near infrared reflectance (NIR-R) fundus images, and spectral domain optical coherence tomography (SD-OCT) scans were acquired during follow-up.

Results—Both patients, aged 45 and 50 years, had good visual acuities (> 20/20 OU) in the context of prolonged dark adaptation. Baseline color fundus photography demonstrated yellow-white, punctate lesions in the temporal macula that correlated with a reticular pattern on FAF and NIR-R imaging. Baseline SD-OCT imaging revealed subretinal deposits that resemble reticular pseudodrusen (RPD) described in age-related macular degeneration (AMD). During follow-up, these affected areas developed confluent thickening of the retinal pigment epithelial (RPE) layer and disruption of the ellipsoid zone of photoreceptors before progressing to overt RPE and outer retinal atrophy.

Conclusions—Structural changes in early stage L-ORD revealed by multimodal imaging resemble those of RPD observed in AMD and other retinal diseases. Longitudinal follow-up of these lesions helps elucidate their progression to frank atrophy and may lend insight into the pathogenic mechanisms underlying diverse retinal degenerations.

Keywords

Late-onset retinal degeneration; Fundus autofluorescence; Optical coherence tomography; Retinal atrophy; Reticular pseudodrusen

Correspondence and Reprint requests to: Catherine Cukras, MD, PhD, Division of Epidemiology and Clinical Applications and Ophthalmic Genetics and Visual Function Branch, National Eye Institute, National Institutes of Health, Bethesda, Maryland 20892, Tel: (301) 435-5061. Fax: (301) 402-1214, cukrasc@nei.nih.gov.

Portions of this work were presented at the 2015 Association for Research in Vision and Ophthalmology (ARVO) meeting

None of the authors has proprietary or financial interests related to the material in this manuscript.

Multi-modal imaging in early Late-onset retinal degeneration reveal findings of reticular pseudodrusen (RPD) which initially occur in the setting of preserved ellipsoid zones (EZ) and over time progress to areas of RPE thickening and detachment with EZ disruption, and then eventually to overt RPE and outer retinal atrophy.

Late-onset retinal degeneration (L-ORD) is an autosomal dominant retinal disease involving the gene encoding C1q and tumor necrosis factor-related protein 5 (C1QTNF5), otherwise known as CTRP5[1, 2]. The disease first presents in the fifth decade of life and generally progresses to bilateral central vision loss by the seventh decade[3]. The earliest clinical findings present as early as the fourth decade and include the prolongation of dark adaptation and abnormalities on iris transillumination, which are related to elongated anterior zonules and peripupillary iris atrophy[2–5]. Patients become symptomatic around the fifth decade, with the most salient complaints of nyctalopia and difficulty adjusting from light to dark conditions. Initial changes on fundus examination involve the appearance of yellow-white drusen-like lesions in the pericentral and midperipheral retina[2–4]. As the disease progresses, scalloped chorioretinal atrophy develops in the temporal retina, which then spreads towards the fovea[6, 7]. Visual acuity is usually preserved until at least the seventh decade when the fovea is compromised by either progressive atrophy or the development of choroidal neovascularization[3, 6, 8].

Histopathological analysis of L-ORD in an 82-year old donor eye has revealed extensive extracellular deposits located between the RPE and Bruch's membrane ranging from the posterior pole to the ora serrata[7]. These deposits were found to be composed of an inner layer containing collagen and mucopolysaccharides and an outer lipid layer. Regional variations in the thickness of the sub-RPE deposit were reported, with the macula and mid-peripheral retina exhibiting the thinnest and thickest deposits, respectively. The extents of photoreceptor loss and RPE thinning were greater in areas with thicker sub-RPE deposits.

More recent studies have characterized autofluorescence and SD-OCT findings in a cross-sectional description of L-ORD patients[4, 6, 9]. Fundus autofluorescence findings include scalloped hypoautofluorescent patches corresponding to areas of chorioretinal atrophy with adjacent areas of speckled hyper- and hypo-autofluorescence[8, 9]. SD-OCT showed sub-RPE deposits with marked disturbances of the photoreceptor outer segments, ellipsoid zone (EZ), and outer nuclear layer (ONL) overlying these areas[9]. Other OCT findings include hyper-reflective deposits, thickening of the RPE/Bruch's membrane complex, triangular hyporeflective spaces with hyperreflective borders at the level of the RPE, and choroidal thinning[9].

This current study describes novel longitudinal observations of L-ORD in two siblings based on multi-modal imaging, which have not to our knowledge been previously reported. These retinal lesions have characteristics of reticular pseudodrusen (RPD) and their progression to retinal atrophy suggests a pathway that may be common to several retinal diseases of different etiologies.

Methods

The patients in this study are enrolled in a protocol at the National Eye Institute, National Institutes of Health (NIH), Bethesda, MD. The protocol was approved by the NIH Institutional Review Board and adheres to the tenets of the Declaration of Helsinki.

Both patients underwent a complete ophthalmoscopic examination including best-corrected visual acuity testing (BCVA), slit lamp examination, and dilated fundus exam. Color fundus photos were acquired with the TRC-50DX retinal camera (Topcon Medical Systems, Oakland, NJ). Fundus autofluorescence (FAF) and near infrared reflectance (NIR-R) fundus images and spectral domain optical coherence tomography (SD-OCT) scans were acquired with the Heidelberg Spectralis (Heidelberg Engineering, Heidelberg, Germany). OCT scans either consisted of 19 B scans, each composed of 14 averaged scans, covering an area of 20° × 15° encompassing the macula; or they consisted of 37 B scans, each composed of 25 averaged scans, covering an area of 30° × 15° encompassing the macula. Patients repeated the ophthalmic studies and imaging studies approximately yearly over the course of 8 years.

Results

The two patients in this study are part of a larger pedigree originally described by Ayyagari and colleagues[3]. Both subjects carry the point mutation S163R in C1QTNF5 in the heterozygous state that has been associated with L-ORD[1], consistent with the genotype of other affected members of this family, and demonstrated typical clinical findings of L-ORD including long anterior lens zonules and delayed dark adaptation[2]. Patient 1 is the male sibling who was 45 years old at the initial baseline visit, while Patient 2 is his sister who was 50 years old at baseline. The best-corrected visual acuity in both patients was 20/20 or better in both eyes of both patients throughout the time followed.

Figure 1 shows the color, FAF, and NIR-R fundus images and an OCT scan for patient 1 at 52 years old. Color imaging (Fig. 1A) reveals yellow-white round punctate lesions roughly equal in size and shape located superotemporal and inferotemporal to the fovea. This same area on FAF (Fig. 1B) demonstrates hypoautofluorescent spots on a background of relative hyperautofluorescence, some of which appear halo-like, and on NIR-R reflectance imaging (Fig. 1C, D), the lesions have hyperreflectant centers with hyporeflectant surrounds (with target-like or halo-like features). An OCT scan (Fig. 1E) corresponding to the green line in Figure 1A reveals the presence of subretinal deposits (asterisks) in the temporal macula with relative preservation of the overlying retinal architecture including the EZ and ONL. In addition, there is no significant separation of the RPE/Bruch's membrane complex, suggesting that significant sub-RPE deposits are not present. These dot-like lesions have the appearance of reticular pseudodrusen on fundus imaging and OCT observed in the setting of AMD. RPD appear clinically as "round, oval, or slightly elongated and lobulated yellowish spots with ill-defined edges, 125μm–250μm in size".[10] AMD-associated RPD also have a pattern of hypo- reflectant/fluorescent or halolike lesions on a background of mildly increased reflectance/fluorescence on NIR-R reflectance and FAF imaging,[11] and they appear as subretinal deposits on SD-OCT[12]. Subtyping of reticular pseudodrusen has been proposed, and in that classification system, these lesions most resemble "dot pseudodrusen" since they appear as white spots on color photographs and have a distinctive target appearance on NIR-R-SLO imaging[13]. OCT also demonstrates diffuse choroidal thinning with a subfoveal choroidal thickness measuring approximately 165 microns or less, which is comparable to the range of choroidal thicknesses seen in a cohort of eyes with RPD in the setting of AMD[14], with mean reported normal central choroidal thickness varying from 330 micron range[15, 16] to 202.6+ 83.5[17].

The longitudinal progression of L-ORD-associated RPD lesions in the macula and temporal retina, the locus where the lesions first appear, was followed in Patient 1 over 4 years (age 49–53 years) (Fig. 2). The green line overlying the NIR-R image in Figure 2A shows the location of the subsequent SD-OCT scans. At age 49 (Fig. 2B), extensive subretinal deposits were observed over the temporal macula but terminated at a defined edge approaching the fovea (arrow in Fig. 2B). Progression of this demarcation line towards the fovea in the temporal-to-nasal direction can be observed (arrows in Figs. 2B, C, and D). Comparing each OCT scan to the one below it, subretinal deposits in the affected temporal zone with previously intact EZ overlying them evolve into conical-shaped accumulations of subretinal material involving the EZ (asterisks in Figs. 2C, D) which resemble stage 3 subretinal drusenoid deposits described in AMD eyes[12]. They later flatten with coincident disruption of the overlying EZ in that area and development of a thickened, hyperreflective RPE/Bruch's membrane complex (white arrowhead Figure 2D). As with nascent subretinal deposits, the pattern of retinal architecture degeneration also follows a temporal-to-nasal progression towards the fovea.

A correlation between the appearance of L-ORD on color, FAF, NIR-R, and OCT imaging for a patient with slightly more advanced findings can be seen in Figure 3, which presents imaging of patient 2 at age 55 years. The color fundus photograph in Figure 3A demonstrates the yellow-white punctate lesions that have been previously described in the early phases of L-ORD and are similar to those shown in patient 1 in Figure 1A. Again, the multimodal imaging reveals findings consistent with RPD lesions characteristic of the previously described "dot" subtype[13], but geographically, they are most apparent in the perifoveal area encircling the fovea in a "c" configuration. Distinct to this patient with more advanced disease, the temporal region of the FAF image also has a mottled appearance with more prominent hyperautofluorescence. Figure 3E is the OCT corresponding to the location of the green line inferior to the fovea in Figure 3A and demonstrates different lesion characteristics across the imaged area. The nasal aspect of the OCT scan demonstrates distinctive subretinal deposits (asterisks), while lesions temporal to the fovea have the appearance of stage 3 RPD that extend from subretinal space into the ONL through the EZ (white arrow). The white arrowhead demarcates the start of an area extending temporally away from the fovea where there is a loss of the distinct subretinal accumulations, and the RPE appears thickened and hyperreflective with a distinct separation between the RPE and Bruch's membrane. Overlying this region, the EZ appears disrupted and mottled, corresponding to the area on FAF (Figure 3B) with mottled hyperautofluorescence.

Longitudinal OCT scans following patient 2 from ages 57 to 59 (Fig. 4) provide further information about the course of progression to advanced disease. OCT scans located inferior to the fovea passing through a temporal area of RPE and photoreceptor loss reveal the temporal-to-nasal gradient observed on FAF. The most nasal portion of the OCT scan appears relatively uninvolved at age 57 (Fig. 4A) but appears to have subretinal accumulations centrally on the scan (inferior to the fovea). Moving temporally, there is thickening of the RPE with separation from Bruch's membrane (temporal to the white arrowhead) and overlying EZ loss (temporal to the white arrow). Finally, the portion of retina temporal to the black arrow demonstrates photoreceptor loss, ONL thinning and frank RPE atrophy, which corresponds spatially to the hypoautofluorescent patches of atrophy on

FAF imaging. Over time (Figs. 4B & C), these changes progress in a temporal-to-nasal direction: the area of RPE separation from Bruch's, again marked with a white arrowhead, and the edges of EZ loss (white arrow) and RPE loss (black arrow) progress towards the fovea with time, as well. The areas where RPE/Bruch's membrane complex has become thickened and hyperreflective, RPE has separated from Bruch's membrane, and the EZ has been lost evolve into the expanse of ONL thinning, RPE loss and choroidal thinning. The correlation of the OCT changes over time with the FAF images suggest that it is the areas with thickened RPE with separation from Bruch's which is predestined to become areas of hypoFAF consistent with RPE and photoreceptor loss.

The changes that are seen to evolve on OCT are also reflected in the progression of the FAF images, which highlight the areas of atrophy. FAF images taken of Patient 2 at ages 50 to 59 show the temporal-to-nasal progression of the reticular pattern on autofluorescence, the extent of which is highlighted by the borders drawn in Figure 5. At 50 and 55 years of age (Figs. 5A & B), the reticular pattern involves the retina superior, temporal, and inferior to the fovea, but by 57 years old (Fig. 5C), it has progressed around the fovea to the area of the macula nasal to the fovea. By age 59 (Fig. 5D), the reticular pattern on autofluorescence completely surrounds the fovea but spares the fovea itself. Hypoautofluorescent patches in the posterior pole and mid-periphery first appear when the patient is 55 years old (highlighted in blue in Figure 5A) and dramatically increase in area over the following 4 years. These patches start as small discrete areas which eventually coalesce. By age 59, temporal-to-nasal progression of atrophy towards the fovea is noted with development of two new areas closer to the fovea. Therefore, it appears that anatomic abnormalities in L-ORD have a predilection to initiate in the temporal macula and progress to encircle the fovea.

Discussion

This study describes disease characteristics and progression in two siblings with L-ORD and demonstrates findings of fundus lesions with characteristics parallel to RPD in the setting of AMD[10, 12, 18–20], and more recently, other retinal degenerations such as Pseudoxanthoma Elasticum (PXE)[21, 22], Sorsby's fundus dystrophy (SFD)[23], Fundus albipunctatus[24], and vitamin A deficiency[25]. While yellow-white, punctate lesions in L-ORD are observed on color imaging, we show here that they appear similar to the "dot" subtype of RPD described by Spaide and colleagues[12, 13].

This longitudinal multi-modality study has enabled us to document the pathophysiology of L-ORD which is a monogenic disease known to initiate with a mutation in the C1QTNF5/CTRP5 gene, which is expressed in the RPE and ciliary epithelium[2, 26, 27]. The protein involved includes an N-terminal signal peptide designating it for secretion, a collagen-like domain that allows monomers to intertwine in a triple helix, and a globular C1q (gC1q) domain placing the protein in the C1q/TNF superfamily[1, 26, 28]. L-ORD patients demonstrate a point mutation c.686 C>G (p.S163R) that is found in the gC1q domain of the protein[1, 2]. Current evidence suggests that the protein may be involved with cell-cell adhesion on the basolateral surface of the RPE[1, 29], although it also localizes to RPE apical

processes[26]. Despite not having a comprehensive understanding of the protein's functions, there is evidence that C1QTNF5 has diverse cellular roles in the RPE.

The resulting implications of mutations in this RPE-expressed gene on the retina that we can appreciate through careful multimodal imaging appear to first manifest in subretinal accumulations (RPD). As the disease progresses, the areas affected by RPD degenerate into regions of thickened, hyperreflective RPE which separates from Bruch's membrane and accumulates sub-RPE material with coincident loss of the overlying photoreceptor EZ. RPE atrophy follows in these areas, and once present, expands rapidly.

Subretinal deposits have not previously been described in L-ORD patients. The availability of longitudinal multi-modal imaging data for these two patients at earlier stages of the disease allowed us to detect events prior to the development of overt atrophy and neovascularization. Two reports of histopathologic findings in L-ORD eye donors at 82 and 80 years old showed choroidal neovascularization, extensive chorioretinal atrophy, and RP-like changes in the periphery[7,6]. They had advanced disease, and therefore it was unlikely that subretinal deposits would have been found. Clinical studies have described fundus findings as drusen-like based upon examination and color imaging. The reticular lesions in this present study could be described as drusen-like based on color fundus photos, but OCT demonstrates their subretinal location. Two recent publications[8, 9] have described FAF and OCT findings in L-ORD that could represent components of the disease progression observed in our patients. Vincent et al. described flecks of hyper- and hypoautofluorescence adjacent to the region of atrophy[8], which may be the same as the mottled autofluorescence in our patient 2. They also mentioned "nodes of thickening of the RPE" over areas of RPE/Bruch's membrane separation[8], which is similar to findings we observed in this study, with separation of the RPE and Bruch's membrane following thickening of the RPE. Soumplis et al. reported focal photoreceptor EZ loss interspersed with regions of EZ preservation, as well as "thickening of the hyper-reflective line corresponding to the RPE/Bruch's membrane complex"[9]. The patients in both studies were older at presentation than the ones in this present study, with the youngest patient in the middle of the sixth decade and most in the seventh or eighth decade of life, and chorioretinal atrophy and choroidal neovascularization were prominent features in most of the eyes.

The information provided by longitudinal, multi-modal imaging presented here allows for the visualization of disease progression in L-ORD that was not previously appreciated. We are proposing a sequence of events that describe the disease progression well before the onset of advanced disease that has implications for the pathogenesis of atrophy in L-ORD. These findings draw many parallels with the RPD phenotype found in AMD although initiate in a different geographic area of the retina – temporal rather than superior macula. In addition to the structural phenotypic commonalities already discussed, evaluation of the OCT reveals choroidal thinning, which has been reported in LORD eyes previously[7, 9], and in our patients choroidal thickness measurements were in the range of those in eyes with RPD in the setting of AMD[14]. Functionally, both L-ORD and AMD with RPD demonstrate similar deficiencies in dark adaptation with prolonged times to reach dimmer thresholds[2, 4, 14] and have a high risk of progression to RPE and outer retinal atrophy[20, 30, 31], as well to the development of choroidal neovascularization (CNV)[3, 32–34].

The recent reports of RPD in PXE and SFD have led to the hypothesis that processes leading to abnormal changes in Bruch's membrane (PXE) or the Bruch's membrane – RPE complex (SFD) contribute to the pathogenesis of RPD[23]. Our cases of patients with early stage L-ORD demonstrating RPD also meet characteristics of being an RPE-based disease that demonstrates RPE thickening and abnormal thickening and accumulations in the Bruch's membrane–RPE complex. Moreover, our longitudinal analysis allows us to observe the sequence of these findings, and, at least within the constraints of SD-OCT resolution, the development of RPD appears to precede the increase in reflectivity and thickness of the RPE and the separation between Bruch's membrane and RPE. These observations lead us to expand upon the previously proposed hypothesis by including RPE, in addition to Bruch's membrane or the Bruch's membrane-RPE interface, as another initiating site where abnormal changes early in the disease course can contribute to the pathogenesis of RPD. Although these retinal degenerations suggest different etiologies for the development of RPD, they share common functional consequences associated with the presence of RPD, including delayed dark adaptation and progression to the development of multi-focal or multi-lobular geographic atrophy[31], although in many cases of Sorsby's and PXE, this may be obscured by the development of CNV. A thickened Bruch's –RPE complex may decrease trophic influences in both directions by (a) decreasing transport of materials from choroid to RPE, and (b) decreasing trophic factors from RPE to choroid. Patterns of degeneration between choroid and RPE may thus be matching in general distribution. Further longitudinal studies of retinal diseases sharing the development of RPD will be necessary to further elucidate the contributions of these factors on disease pathogenesis.

The parallels in the anatomic and functional changes that accompany these findings of RPD, which span several different retinal diseases, support the possibility of a common pathway of photoreceptor dysfunction, death and progression to atrophy.

Acknowledgments

We'd like to thank our patients and their families for their dedication to clinical research.

This work has been supported by the National Eye Institute Intramural Research Program. Portions of this research was made possible through the National Institutes of Health (NIH) Medical Research Scholars Program, a public-private partnership supported jointly by the NIH and generous contributions to the Foundation for the NIH from Pfizer Inc, The Doris Duke Charitable Foundation, The Alexandria Real Estate Equities, Inc. and Mr. and Mrs. Joel S. Marcus, and the Howard Hughes Medical Institute, as well as other private donors.

References

1. Hayward C, et al. Mutation in a short-chain collagen gene, CTRP5, results in extracellular deposit formation in late-onset retinal degeneration: a genetic model for age-related macular degeneration. Hum Mol Genet. 2003; 12:2657–2667. [PubMed: 12944416]
2. Ayyagari R, et al. Late-onset macular degeneration and long anterior lens zonules result from a CTRP5 gene mutation. Invest Ophthalmol Vis Sci. 2005; 46:3363–3371. [PubMed: 16123441]
3. Ayyagari R, et al. Autosomal dominant hemorrhagic macular dystrophy not associated with the TIMP3 gene. Arch Ophthalmol. 2000; 118:85–92. [PubMed: 10636420]
4. Jacobson SG, et al. Phenotypic marker for early disease detection in dominant late-onset retinal degeneration. Invest Ophthalmol Vis Sci. 2001; 42:1882–1890. [PubMed: 11431457]
5. Subrayan V, et al. Long anterior lens zonules in late-onset retinal degeneration (L-ORD). Am J Ophthalmol. 2005; 140:1127–1129. [PubMed: 16376663]

6. Kuntz CA, et al. Sub-retinal pigment epithelial deposits in a dominant late-onset retinal degeneration. Invest Ophthalmol Vis Sci. 1996; 37:1772–1782. [PubMed: 8759344]
7. Milam AH, et al. Dominant late-onset retinal degeneration with regional variation of sub-retinal pigment epithelium deposits, retinal function, and photoreceptor degeneration. Ophthalmology. 2000; 107:2256–2266. [PubMed: 11097607]
8. Vincent A, et al. The characterization of retinal phenotype in a family with C1QTNF5-related late-onset retinal degeneration. Retina. 2012; 32:1643–1651. [PubMed: 22277927]
9. Soumplis V, et al. Phenotypic findings in C1QTNF5 retinopathy (late-onset retinal degeneration). Acta Ophthalmol. 2013; 91:e191–195. [PubMed: 23289492]
10. Arnold JJ, et al. Reticular pseudodrusen. A risk factor in age-related maculopathy. Retina. 1995; 15:183–191. [PubMed: 7569344]
11. Ooto S, et al. Reduction of retinal sensitivity in eyes with reticular pseudodrusen. Am J Ophthalmol. 2013; 156:1184–1191 e1182. [PubMed: 23972310]
12. Zweifel SA, et al. Reticular pseudodrusen are subretinal drusenoid deposits. Ophthalmology. 2010; 117:303–312 e301. [PubMed: 19815280]
13. Suzuki M, Sato T, Spaide RF. Pseudodrusen subtypes as delineated by multimodal imaging of the fundus. Am J Ophthalmol. 2014; 157:1005–1012. [PubMed: 24503406]
14. Flamendorf J, et al. Impairments in Dark Adaptation Are Associated with Age-Related Macular Degeneration Severity and Reticular Pseudodrusen. Ophthalmology. 2015
15. Spaide RF, Koizumi H, Pozzoni MC. Enhanced depth imaging spectral-domain optical coherence tomography. Am J Ophthalmol. 2008; 146:496–500. [PubMed: 18639219]
16. Rahman W, et al. Repeatability of manual subfoveal choroidal thickness measurements in healthy subjects using the technique of enhanced depth imaging optical coherence tomography. Invest Ophthalmol Vis Sci. 2011; 52:2267–2271. [PubMed: 21087970]
17. Hirata M, et al. Macular choroidal thickness and volume in normal subjects measured by swept-source optical coherence tomography. Invest Ophthalmol Vis Sci. 2011; 52:4971–4978. [PubMed: 21622704]
18. Smith RT, et al. Autofluorescence characteristics of early, atrophic, and high-risk fellow eyes in age-related macular degeneration. Invest Ophthalmol Vis Sci. 2006; 47:5495–5504. [PubMed: 17122141]
19. Smith RT, et al. Reticular macular disease. Am J Ophthalmol. 2009; 148:733–743 e732. [PubMed: 19878758]
20. Zweifel SA, et al. Prevalence and significance of subretinal drusenoid deposits (reticular pseudodrusen) in age-related macular degeneration. Ophthalmology. 2010; 117:1775–1781. [PubMed: 20472293]
21. Gliem M, et al. Reticular pseudodrusen associated with a diseased bruch membrane in pseudoxanthoma elasticum. JAMA Ophthalmol. 2015; 133:581–588. [PubMed: 25764262]
22. Zweifel SA, et al. Multimodal fundus imaging of pseudoxanthoma elasticum. Retina. 2011; 31:482–491. [PubMed: 20966826]
23. Gliem M, et al. Reticular Pseudodrusen in Sorsby Fundus Dystrophy. Ophthalmology. 2015
24. Genead MA, Fishman GA, Lindeman M. Spectral-domain optical coherence tomography and fundus autofluorescence characteristics in patients with fundus albipunctatus and retinitis punctata albescens. Ophthalmic genetics. 2010; 31:66–72. [PubMed: 20450307]
25. Aleman TS, Garrity ST, Brucker AJ. Retinal structure in vitamin A deficiency as explored with multimodal imaging. Documenta ophthalmologica Advances in ophthalmology. 2013; 127:239–243. [PubMed: 23900584]
26. Mandal MN, et al. CTRP5 is a membrane-associated and secretory protein in the RPE and ciliary body and the S163R mutation of CTRP5 impairs its secretion. Invest Ophthalmol Vis Sci. 2006; 47:5505–5513. [PubMed: 17122142]
27. Chavali VR, et al. A CTRP5 gene S163R mutation knock-in mouse model for late-onset retinal degeneration. Hum Mol Genet. 2011; 20:2000–2014. [PubMed: 21349921]
28. Kishore U, et al. C1q and tumor necrosis factor superfamily: modularity and versatility. Trends Immunol. 2004; 25:551–561. [PubMed: 15364058]

29. Alten F, et al. Characterisation of reticular pseudodrusen and their central target aspect in multi-spectral, confocal scanning laser ophthalmoscopy. Graefes Arch Clin Exp Ophthalmol. 2014; 252:715–721. [PubMed: 24276561]

30. Marsiglia M, et al. Association between geographic atrophy progression and reticular pseudodrusen in eyes with dry age-related macular degeneration. Invest Ophthalmol Vis Sci. 2013; 54:7362–7369. [PubMed: 24114542]

31. Xu L, et al. Reticular macular disease is associated with multilobular geographic atrophy in age-related macular degeneration. Retina. 2013; 33:1850–1862. [PubMed: 23632954]

32. Cohen SY, et al. Prevalence of reticular pseudodrusen in age-related macular degeneration with newly diagnosed choroidal neovascularisation. Br J Ophthalmol. 2007; 91:354–359. [PubMed: 16973663]

33. Pumariega NM, et al. A prospective study of reticular macular disease. Ophthalmology. 2011; 118:1619–1625. [PubMed: 21550118]

34. Aye KH, et al. Treatment of a choroidal neovascular membrane in a patient with late-onset retinal degeneration (L-ORD) with intravitreal ranibizumab. Eye (Lond). 2010; 24:1528–1530.

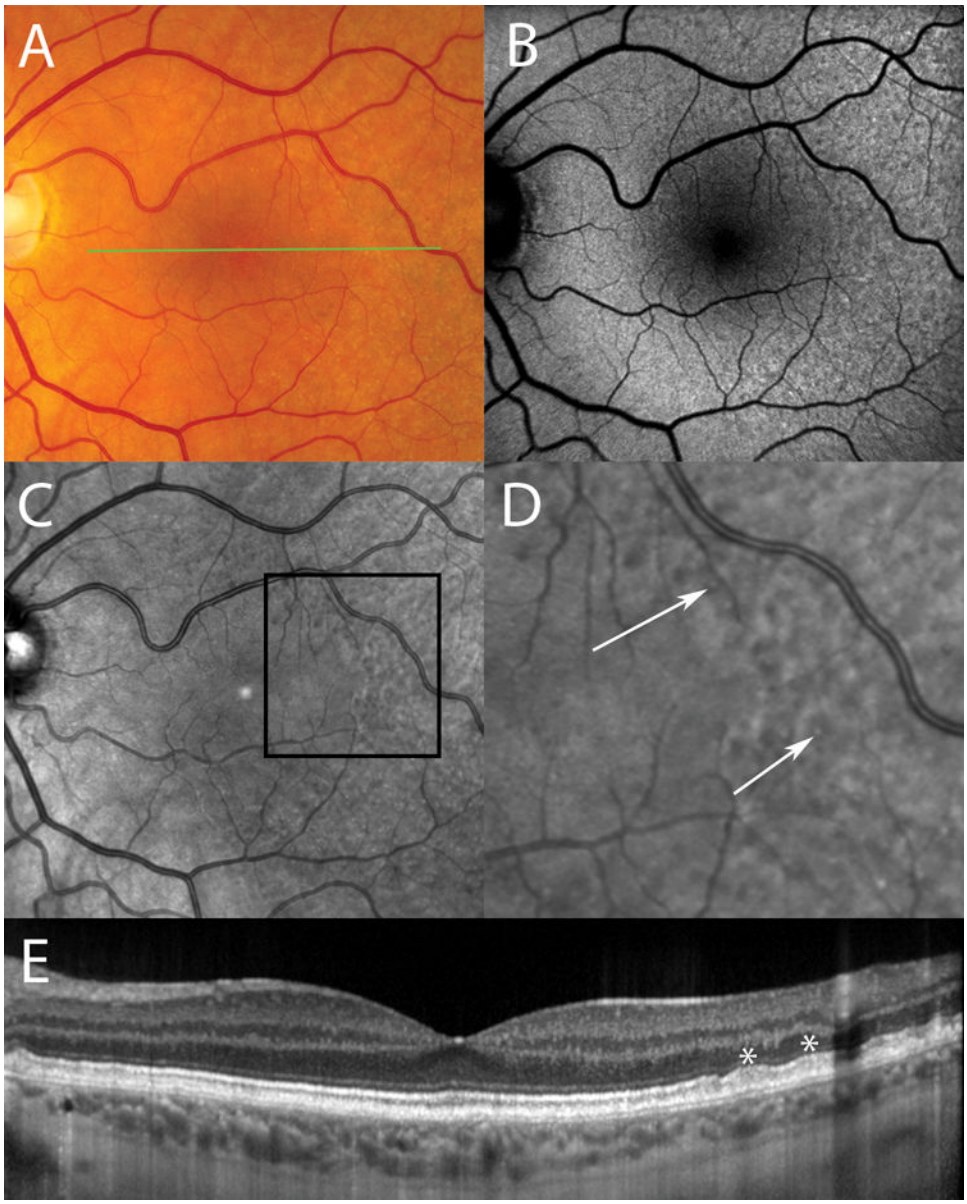

Figure 1.

Multi-modal imaging of the left eye of patient 1 at 52 years old. **(A)** Punctate yellow-white lesions of roughly equal size and shape are visible superotemporal and inferotemporal to the fovea on color fundus photography. **(B**) Fundus autofluorescence imaging demonstrates hypoautofluorescent spots on a background of mildly elevated hyperautofluorescence. **(C)** Infrared reflectance reveals hyporeflectant lesions with hyperreflectant cores, and a magnified view of the region within the black box can be seen in **(D)**, with the white arrows highlighting two examples of these lesions. The horizontal green line in **(A)** shows the location of the OCT scan shown in **(E)**. The white stars are located above subretinal deposits in the temporal macula.

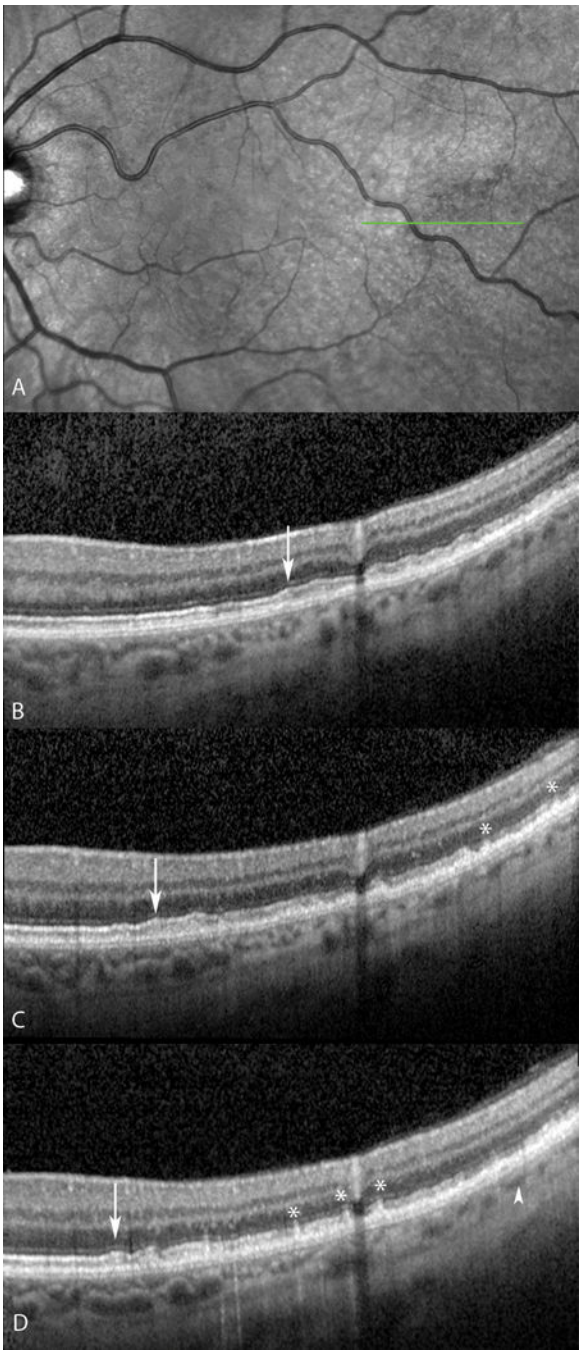

Figure 2.

Progression of retinal pathology viewed with OCT in left eye of patient 1. **(A)** Infrared reflectance image shows the temporal location corresponding to the OCT scans taken when the patient was 49 years old **(B)**, 52 years old **(C)**, and 53 years old **(D)**. The white arrows mark the foveal extent of the subretinal deposits at each timepoint; demonstrating geographic progression (temporal-to-nasal) of these lesions. The temporal portion of **(B)** shows the presence of subretinal deposits (consistent with RPD) with an overlying intact ellipsoid zone (EZ). Longitudinal followup of these lesions in **(C)** and **(D)** demonstrate the

temporal progression of the subretinal lesions in this area to more conical subretinal lesions with overlying EZ loss, indicated with white asterisks, which are morphologically similar to a stage 3 RPD. The white arrowhead in **(D)** highlights the development of hyperreflective and thickened RPE.

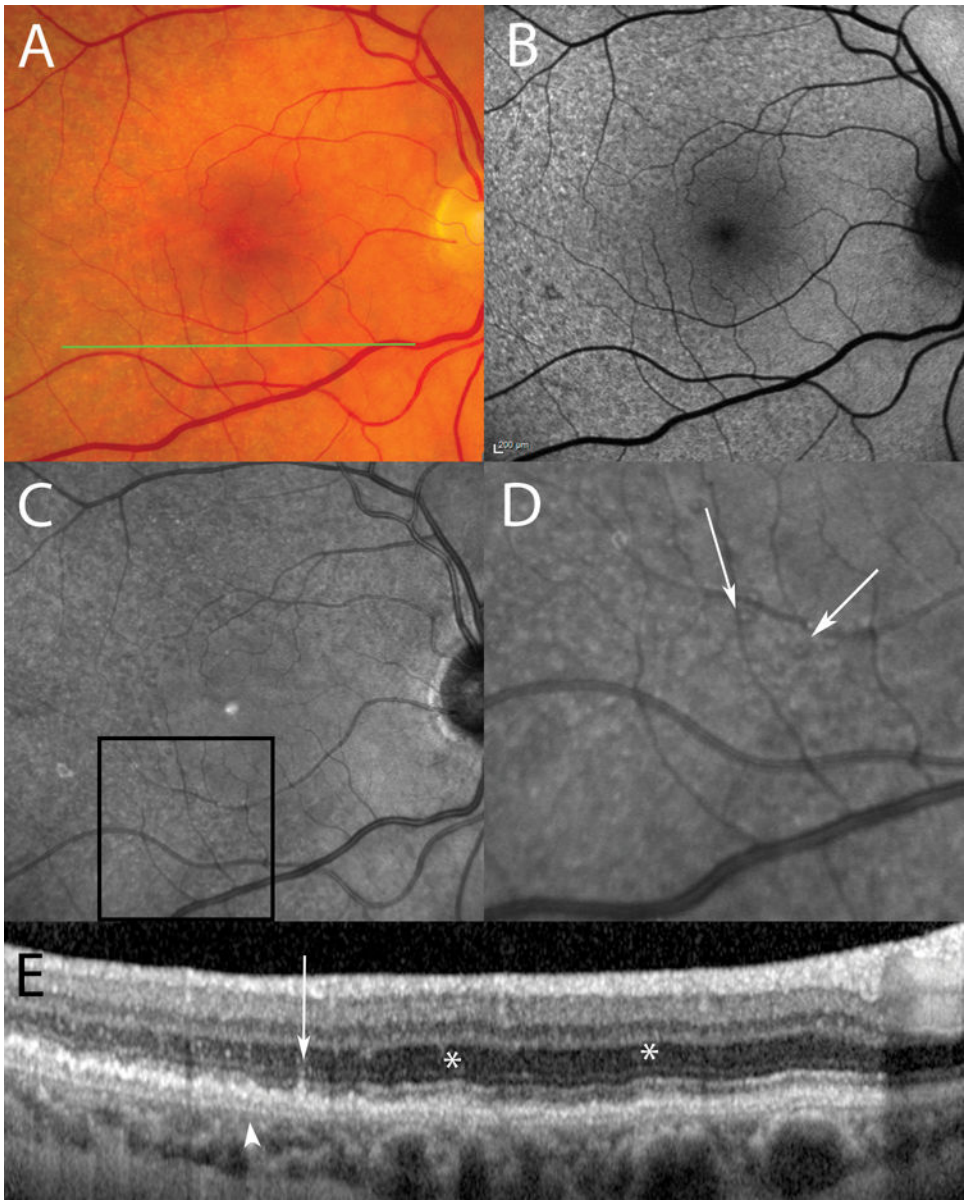

Figure 3.

Multi-modal imaging of the right eye of patient 2 at 55 years old. **(A)** Punctate yellow-white lesions of roughly equal size and shape are visible superior, inferior and temporal to the fovea on color fundus photography. **(B**) Fundus autofluorescence imaging demonstrates two regions of autofluorescent characteristics. The temporal retina demonstrates a mottled appearance of hyper and hypoautofluorescent areas. The perifoveal retina appears to have more distinct hypoautofluorescent lesions resembling the halo-like appearance of RPD. **(C)** Infrared reflectance reveals hyporeflectant lesions with hyperreflectant cores in the perifoveal area, and a magnified view of the region within the black box can be seen in **(D)**, with the white arrows highlighting two examples of these lesions. The horizontal green line in **(A)** shows the location of the OCT scan shown in **(E)**. The white stars are located above subretinal deposits in the temporal retina, similar to the appearance of stage 2 RPD while the

white arrow marks a more canonical subretinal lesion interrupting the EZ that is similar to a stage 3 RPD. The white arrowhead marks an area of RPE thickening and hyperreflectance and a separation of the RPE from Bruch's membrane.

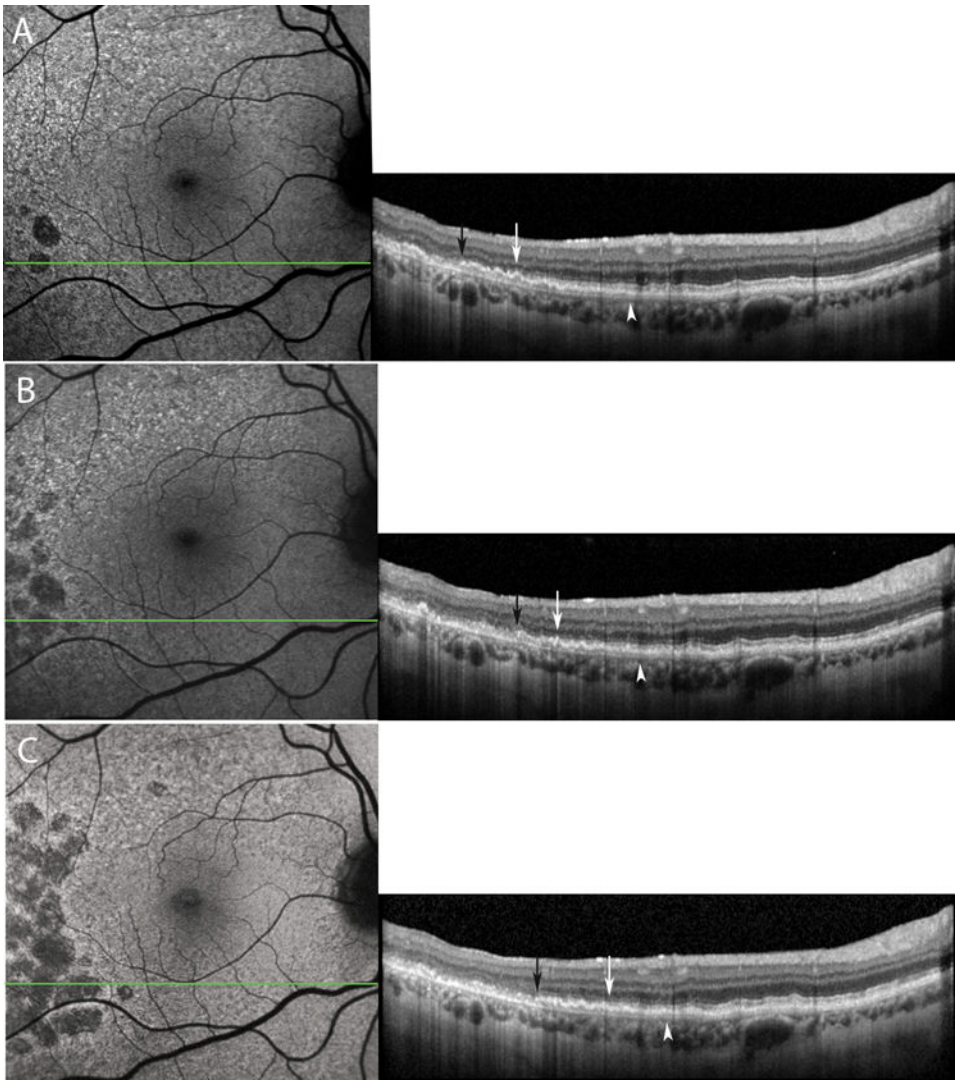

Figure 4.

Progression of retinal pathology on FAF and OCT in right eye of patient 2. The green lines on the FAF images mark the location corresponding to the serial OCT scans taken when the patient was 57 years old **(A)**, 58 years old **(B)**, and 59 years old **(C)**. The arrowheads mark the point at which the RPE can be seen to separate from Bruch's membrane and become thickened and hyperreflective. The white arrow marks the most temporal extent that the EZ can be observed to extend. The black arrows indicate the temporal aspect of the presence of the RPE layer temporal to which there is discontinuity of the RPE band correlating to an area of hypoautofluorescence on the FAF image. There is a progression of these points as they march nasally over time with progression of the disease.

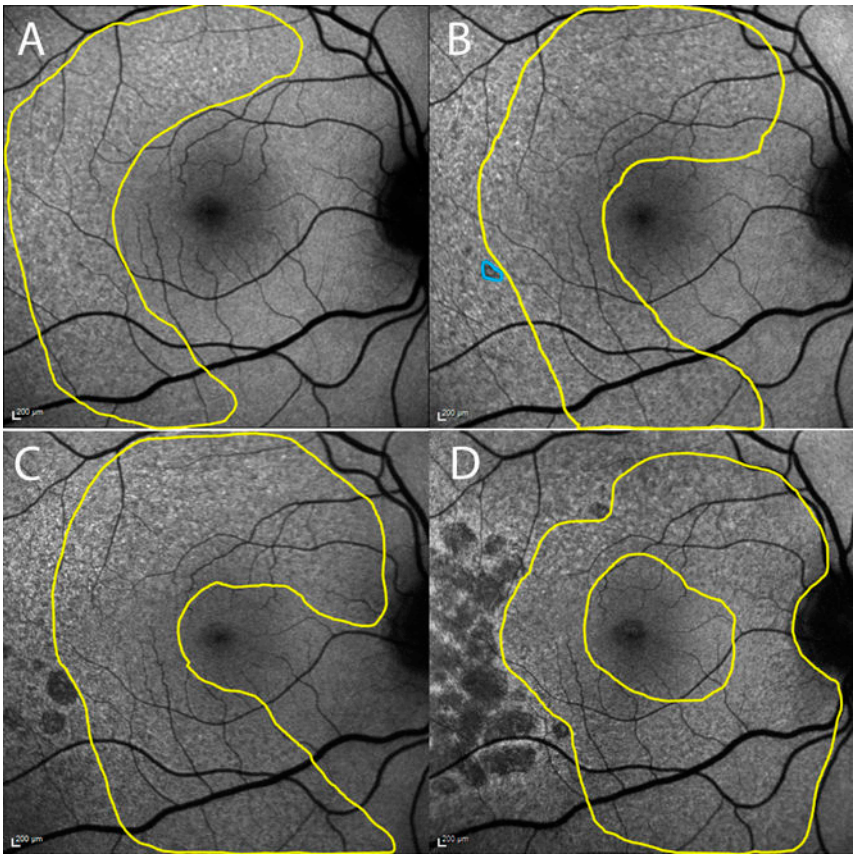

Figure 5.

Progression of retinal pathology viewed with FAF in the right eye of patient 2 taken over 9 years at ages 50 **(A)**, 55 **(B)**, 57 **(C)**, and 59 **(D)**. The yellow line encircles the area of reticular pattern consistent with RPD. This area appears to march towards the fovea, but spares the fovea as the reticular pattern encircles the fovea. In the temporal macula, there is evolution of a small patch of atrophy (blue) which rapidly expands over the next 4 years (hypofluorescent lesions in C and D).